

Spin dimers in the quantum ferrimagnet $\text{Cu}_2\text{Fe}_2\text{Ge}_4\text{O}_{13}$ under staggered and random magnetic fields

T. Masuda*

Department of Nanosystem Science, Yokohama City University, Yokohama, Kanagawa 236-0027, Japan

K. Kakurai

Quantum Beam Science Division, JAEA, Tokai, Ibaraki 319-1195, Japan

A. Zheludev†

Institute for Solid State Physics, ETH, CH-8093 Zürich, Switzerland and Laboratory for Neutron Scattering, ETH and Paul Scherrer Institut, CH-5232 Villigen PSI, Switzerland

(Received 13 September 2009; published 12 November 2009)

We study $S=1/2$ dimer excitation in a coupled chain and dimer compound $\text{Cu}_2\text{Fe}_2\text{Ge}_4\text{O}_{13}$ by inelastic neutron-scattering technique. The Zeeman split of the dimer triplet by a staggered field is observed at low temperature. With the increase in temperature, the effect of a random field is detected by a drastic broadening of the triplet excitation. Basic dynamics of dimer in the staggered and random fields are experimentally identified in $\text{Cu}_2\text{Fe}_2\text{Ge}_4\text{O}_{13}$.

DOI: [10.1103/PhysRevB.80.180412](https://doi.org/10.1103/PhysRevB.80.180412)

PACS number(s): 75.10.Jm, 75.25.+z, 75.50.Ee

Excitations in quantum spin liquids can be viewed as strongly interacting bosonic quasiparticles. This circumstance enables experimental studies of the physics of Bose liquids in prototypical quantum magnetic materials.¹⁻³ Such experiments are often possible under conditions that cannot be realized in more conventional models such as ^4He (Refs. 4 and 5) and ultracold trapped ions.^{6,7} One recent topic of interest is the behavior of bosonic quasiparticles in the presence of disorder. Phases, such as the random singlet state⁸ and Bose and Mott glasses,⁹ have been predicted for systems with quenched disorder. In real prototype materials, one usually tries to create such disorder by chemical doping.^{10,11} In the present work, we demonstrate an alternative approach: a random magnetic field created by disordered (paramagnetic) ions. We show that such a random field acting on a simple dimer-based quantum spin liquid dramatically alters the excitation spectrum.

Let us consider the effect of different types of magnetic fields on an isolated $S=1/2$ dimer, as shown in Fig. 1. In a uniform field, the excited triplet is split into three levels. Eventually, at high field, $|S=1, S^z=0\rangle$ will cross the singlet ground state. In the presence of interdimer interactions, BEC of magnon will occur. If local fields applied to each dimer spin are antiparallel to each other (referred to as “staggered field” hereafter), the triplet is split into a singlet and a doublet. The singlet ground state becomes mixed with $|S=1, S^z=0\rangle$ and the total spin is no longer a good quantum number. Even in an infinitesimal staggered field, the ground state becomes polarized. Now, if the field direction is spatially randomized, each dimer will experience both a staggered and uniform component. The corresponding energy levels can be calculated numerically. The resulting density of state (DOS) for excitations in a set of N dimers is plotted in the right panel in Fig. 1. The lower and higher boundaries of the DOS spread coincide with the levels of $|S_z=1\rangle$ and $|S_z=-1\rangle$ in the uniform field.

The quantum ferrimagnet $\text{Cu}_2\text{Fe}_2\text{Ge}_4\text{O}_{13}$ (Ref. 12) is a

rare potential realization of this random-field effect. The compound includes $S=1/2$ Cu^{2+} dimers coupled to classical Fe^{3+} chains.¹³ At low temperature, the cooperative ordered state with classical spin and quantum spin is stabilized by a weak intersubsystem coupling. In the adiabatic approximation, the quantum spins are effectively under the internal field from the much slower fluctuating classical spins. In this compound, the staggered nature of the exchange field is due to the magnetic structure. The staggered magnetization curves of dimers in $\text{Cu}_2\text{Fe}_2\text{Ge}_4\text{O}_{13}$ (Ref. 14) were experimentally obtained by measuring the temperature dependence of sublattice moments in neutron diffraction. At high temperature, in the paramagnetic phase, the classical spins are thermally disordered and the effective field on the quantum spins is randomly oriented. Then the system can be considered as the ensemble of N dimers in a random quasistatic field. As shown in Fig. 1, the effect of this random field is to broaden the dimer excitations at $T > T_N$.

In the previous inelastic neutron-scattering study, it was shown that the energy scales of excitations in the Fe chains and Cu dimers are well separated.^{13,15} The lower-energy excitations up to 10 meV are Fe-based spin waves. Preliminary powder experiments¹³ and comparative studies in an isostructural compound $\text{Cu}_2\text{Sc}_2\text{Ge}_4\text{O}_{13}$ (Ref. 16) associated the dispersionless excitations at 24 meV with Cu dimers. How-

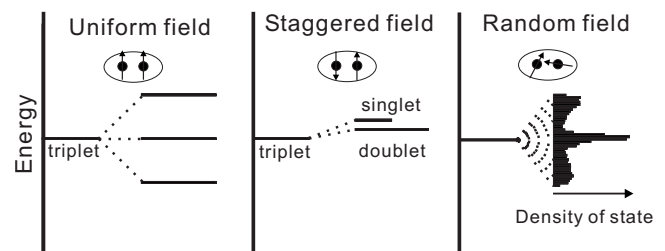


FIG. 1. Schematic diagrams of triplet excitations in $S=1/2$ dimers in different types of locally applied magnetic field.

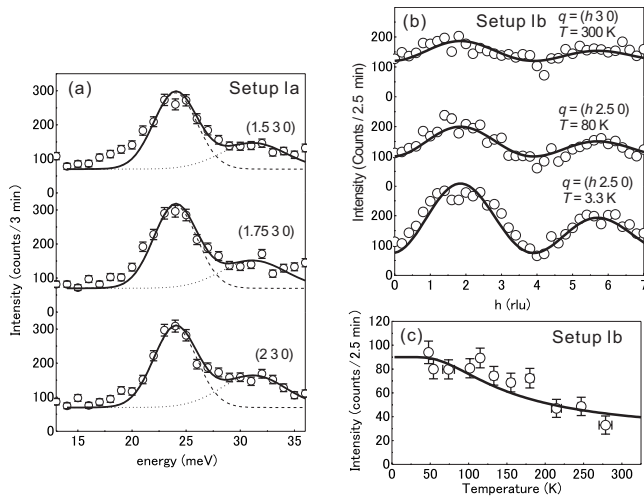


FIG. 2. Inelastic neutron scattering using experimental setups Ia and Ib. (a) Typical energy scans at $(h k 0)$. Dispersionless excitations are observed at $\hbar\omega=24$ and 31 meV. Two peaks are separately fit by Gaussians (dotted curves). (b) h scans at $\hbar\omega=24$ meV at various temperatures. Sinusoidal intensity modulations are fitted to the dimer structure factor calculated for zero field plus a constant background (solid curves). (c) Temperature dependence of the peak intensity at $q=(h 2.5 0)$ and $\hbar\omega=24$ meV.

ever, the effect of a staggered and/or fluctuating field could not be identified in powder samples. In this Rapid Communication, we study the dimer excitations by single-crystal inelastic neutron scattering. By adopting a high-resolution setup, we identify the split peaks due to the staggered exchange field. Furthermore, we observe a drastic broadening of the peak profile at $T > T_N$ that can be ascribed to randomly oriented field from thermally fluctuated Fe moments.

High quality single crystals were grown by the floating-zone method. The crystals (monoclinic $P2_1/m$) were found to be twinned, so that both microscopic domains share a^*-b^* plane. To avoid complications due to twinning, we restrict the measurements to the a^*-b^* plane. In the setups, Ia and Ib Pyrolytic Graphite (PG) (002) were used for both monochromator and analyzer. The Soller collimations were $48'-60'-60'-120'$ and open- $80'-80'$ -open for Ia and Ib, respectively. In setup II, to achieve high-energy resolution, PG (004) for monochromator and PG (002) for analyzer with $30'-20'-40'-120'$ were used. The setups Ia and II were performed on HB1 spectrometer in HFIR (ORNL). The setup Ib was performed on TAS1 spectrometer in JRR-3M (JAEA). In all setups, the final energy of the neutron was fixed at $E_f = 14.7$ meV and PG filter was installed after the sample to eliminate higher-order contamination. A closed cycle He refrigerator was used to achieve low temperatures.

In a series of energy scans in a wide range of $(h k 0)$ space shown in Fig. 2(a), two dispersionless peaks are readily identified: a pronounced one at $\hbar\omega \sim 24$ meV and a weaker feature at $\hbar\omega \sim 31$ meV. The experiments were performed in setups Ia and Ib. The former is consistent with the Cu-centered magnetic excitation in previous studies.^{13,16} Constant energy scan at $\hbar\omega=24$ meV and its temperature dependence are shown in Fig. 2(b). The observed sinusoidal intensity modulation is characteristics of dimer excitations

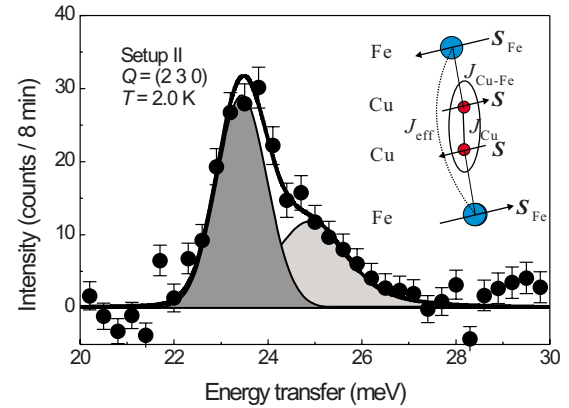


FIG. 3. (Color online) Energy scan collected using the high-resolution setup II at $T=2.0$ K. The shoulder structure is reproduced by the doublet (shaded with white background) and singlet (shaded with gray background) dimer excitations split by a staggered exchange field.

and is observed in a wide temperature range. In Fig. 2(c), the temperature dependence of the peak intensity is shown. The intensity at $q=(0 2.5 0)$ was measured at each temperature and then subtracted as background. The decrease in the intensity at high temperature is common behavior for magnetic excitations in local spin clusters. The smaller peak at $\hbar\omega \sim 31$ meV was identified as a Fe-centered excitation, as will be discussed below.

To obtain a more detailed profile, we performed an energy scan using setup II at $T=2.0$ K. As shown in Fig. 3, it is revealed that the primary peak at $\hbar\omega=24$ meV actually has a shoulder structure. The main peak is located at 23.5 meV, and a smaller bump is centered around 25.0 meV. This splitting is attributed to the staggered exchange field from the adjacent Fe moments. The main peak corresponds to the excitation doublet and the small one to the singlet.

Energy scans collected at several temperatures are shown Fig. 4(a). The small peak at $\hbar\omega \sim 31$ meV in Fig. 2 is temperature independent and has been subtracted from the data. Well-defined peaks are observed at all temperatures. While at low temperature the peak profile is sharp and the width is within resolution limit, at $T \geq T_N$ the peak becomes drastically broadened. This qualitative behavior is consistent with the effect a random exchange field should have on the dimer excitation triplet. The data were analyzed using Gaussian fits. The estimated peak positions, widths, and the integrated intensities are plotted as functions of temperature in Figs. 4(b)–4(d). With increasing temperature, the peak energy decreases at $T \sim T_N$ and stays constant beyond. The peak width drastically increases at $T \sim T_N$ but also remains constant at higher temperature. The integrated intensity decreases by 10–20%. It is noted that in the previous powder experiment, the peak cannot be distinguished at $T \geq 41$ K.¹³ This is because the powder integration in wide q space collects phonon excitations and accidental spurious peaks, masking magnetic excitations at higher temperatures.

For $T < T_N$, we will consider the following effective Hamiltonian:

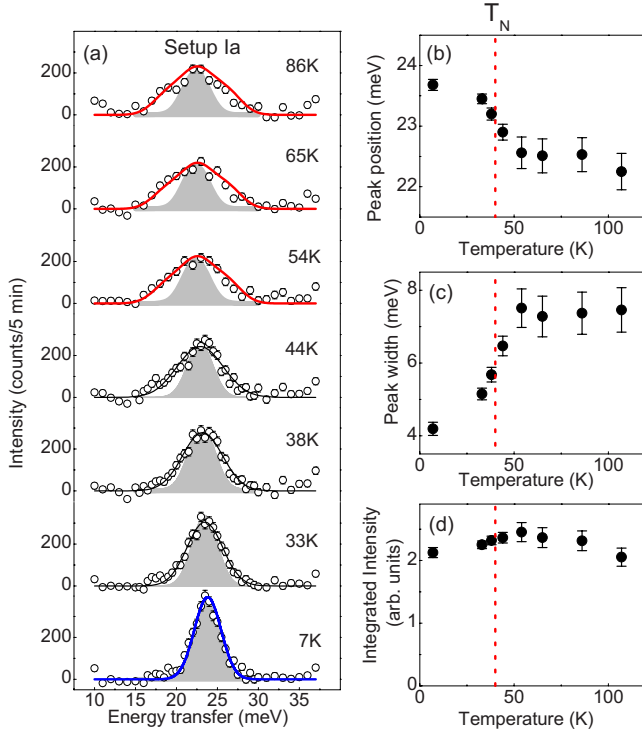


FIG. 4. (Color online) (a) Temperature dependence of the peak profile at $\mathbf{q}=(2\ 3\ 0)$. Experimental resolution is indicated by the gray area. Small peaks due to Fe-centered excitation at 31 meV are separately fitted and subtracted. Profiles at $T \geq 54$ K are reproduced by dimers in a randomly oriented field model (solid curves). The temperature dependence of peak positions (b), widths (c), and integrated intensities (d), as estimated from Gaussian fits.

$$H = J_{\text{Cu}} \mathbf{S}_1 \cdot \mathbf{S}_2 + g\mu_B \mathbf{S}_1 \cdot \mathbf{h}_1 + g\mu_B \mathbf{S}_2 \cdot \mathbf{h}_2, \quad (1)$$

where $\mathbf{h}_1=(0\ 0\ h)$ and $\mathbf{h}_2=(0\ 0\ -h)$. Here the z axis is chosen along the ordered Cu moment. The ground-state energy E_G decreases with the field $E_G = -J_{\text{Cu}}/4 - \sqrt{(2g\mu_B h)^2 + J_{\text{Cu}}^2}/2$, and the excitation triplet splits into a singlet and doublet. The corresponding energy levels are given by

$$\Delta_s = \sqrt{(2g\mu_B h)^2 + J_{\text{Cu}}^2}, \quad (2)$$

$$\Delta_d = J_{\text{Cu}}/2 + \sqrt{(2g\mu_B h)^2 + J_{\text{Cu}}^2}/2, \quad (3)$$

and plotted vs h in Fig. 1. For $g\mu_B h \ll \Delta$, the neutron cross section is approximately given by

$$\begin{aligned} \frac{d^2\sigma}{d\Omega dE} &\sim N(\gamma r_0)^2 \frac{k'}{k} \sin^2(\mathbf{q} \cdot \mathbf{d}) [f(q)]^2 P(T) \{A(h) \\ &\times (1 + \cos^2 \theta) \delta(\hbar\omega - \Delta_d) + B(h) \sin^2 \theta \delta(\hbar\omega - \Delta_s)\}. \end{aligned} \quad (4)$$

The doublet and singlet terms correspond to transverse and longitudinal spin fluctuations, respectively. $A(h)$ and $B(h)$ are h -dependent parameters with $A(h) \leq 1$, $B(h) \leq 1$ and $A(0)=B(0)=1$. Since the staggered field stabilizes the polarized spin configuration and suppresses longitudinal fluctuation, $B(h)$ decrease with h . Meanwhile, $A(h)$ is almost con-

stant in the low field. $P(T)$ is a temperature factor $P(T) = 1/\{1 + 2 \exp(-\beta\Delta_d) + \exp(-\beta\Delta_s)\}$. \mathbf{q} is the scattering vector, \mathbf{d} is the spin separation in each dimer, and θ is the angle between \mathbf{q} and the moment of Cu. We used $\mathbf{m}_{\text{Cu}} = (-0.227, 0.035, -0.301)\mu_B$ (Ref. 14) to calculate θ . Two types of domains, namely, antiferromagnetic and crystallographic ones due to twinning, are considered.

The peak profile in Fig. 3 is reasonably well reproduced by the cross section convoluted by experimental resolution function with $\Delta_s = 25.0$ meV and $\Delta_d = 23.5$ meV. From Eqs. (2) and (3), $J_{\text{Cu}} = 22.0$ meV and $h = 51$ T are obtained. Let us check the consistency of h with the previous study.¹⁴ From the staggered magnetization curve by neutron diffraction, $J_{\text{Cu-Fe}}/J_{\text{Cu}} = 0.105$ was obtained. Here $J_{\text{Cu-Fe}}$ is the interaction between Cu and Fe spins. Using the molecular-field relation $h = m_{\text{Fe}} J_{\text{Cu-Fe}} / (g\mu_B)^2$ and previously obtained parameters, $h \sim 40$ T is estimated. Thus, the statically estimated value is consistent with that obtained in the present dynamic measurement.

The energy splitting between the singlet and doublet states is about 1.5 meV. This value is small compared with the energy resolution in the typical experimental setup. In the setup, Ia and Ib at $T < T_N$, therefore, staggered field effect is smeared and two terms in Eq. (4) are integrated. Then the cross section is approximately equivalent to that at $h=0$. Indeed, the constant energy scan at $T=3.3$ K in Fig. 2(b) is reasonably fitted by dimers cross section in zero field shown by the thick curve.

At $T > T_N$, effective field on the Cu dimers is randomly oriented. We consider an ensemble of N dimers in random field. The randomly oriented field \mathbf{h} is assumed to have a constant magnitude in Eq. (1). The resulting DOS of the excited states is then calculated numerically. The neutron cross section is assumed to be approximately proportional to the DOS,

$$\frac{d^2\sigma}{d\Omega dE} = (\gamma r_0)^2 \frac{k'}{k} \sin^2(\mathbf{q} \cdot \mathbf{d}) f(q)^2 P_{\text{rand}}(T) D(\hbar\omega), \quad (5)$$

with $\int D(\epsilon) d\epsilon = 3N$ and $P_{\text{rand}}(T) = N/[N + \int D(\epsilon) e^{-\epsilon/k_B T} d\epsilon]$. The data collected at $T \geq 54$ K are well reproduced by this cross section convoluted by the experimental resolution function, as indicated by solid curves in Fig. 4(a). The obtained fit parameters are $J_{\text{Cu}} = 22.3(4)$ meV and $h = 41.8(8)$ T. The values are reasonably consistent with those obtained at $T \leq T_N$. The \mathbf{q} dependence of the cross section is the same as for zero field and is given by the dimer structure factor $\sin^2(\mathbf{q} \cdot \mathbf{d})$. Indeed, the \mathbf{q} scans at 80 and 300 K in Fig. 2(b) are reproduced by this model. The temperature dependence in Fig. 2(c) is well accounted for by the temperature factor $P_{\text{rand}}(T)$.

We shall now discuss the small decrease in the intensity at $T < T_N$ in Fig. 4(d). At $T > T_N$, dimer spins are fluctuated equally in all directions and the dynamical spin correlation is fully detected by neutron. In the ordered state, the polarized magnetic ordering suppresses the longitudinal fluctuation of Cu spins. To estimate the reduction in the longitudinal excitation, we calculate $B(h=51\text{ T}) = 0.77$. The reduction in $B(h)$ is about 20% that is consistent with the experiment. This means that 51 T is rather modest compared with the in-

trimer interaction $J_{\text{Cu}}=22$ meV. If the effective field was large and the moment was fully polarized, the suppression would be more drastic. Such a situation is in fact realized in Haldane spin chains coupled to the rare-earth moment in $\text{Pr}_2\text{BaNiO}_5$ with fully saturated Ni^{2+} moment at $T < T_N$.¹⁷ The Haldane-gap mode lost half of its intensity at $T < T_N$ and it was ascribed to the total suppression of longitudinal mode.

Finally, we will mention the temperature-independent small peak at $\hbar\omega \sim 31$ meV in Fig. 2(a). If the Fe $S=5/2$ chains were perfectly isolated from the Cu subsystem, the Fe excitation spectrum would be dominated by one-magnon excitation at $\hbar\omega \leq 5J_{\text{Fe}}$. However, a recent theory predicts that the introduction of Cu dimer enhances the multimagnon excitation of Fe spins at $\hbar\omega = 10J_{\text{Fe}}$, $15J_{\text{Fe}}$, $20J_{\text{Fe}}$, and $25J_{\text{Fe}}$. According to the Bond operator method,^{18,19} the excitation at $\hbar\omega = 20J_{\text{Fe}}$ is the particularly enhanced.²⁰ Since $J_{\text{Fe}} = 1.6$ meV,¹⁵ the observed small peak at $\hbar\omega = 31$ meV could be ascribed to the Fe-centered longitudinal excitation. Further details will be published somewhere else.

To conclude, we have experimentally investigated the dynamics of $S=1/2$ dimers in staggered and random fields in $\text{Cu}_2\text{Fe}_2\text{Ge}_4\text{O}_{13}$. The staggered field is realized at $T < T_N$ and produces a splitting of the excitation triplet. At $T > T_N$, a random exchange field produces a drastic broadening of these modes. In the future, polarized neutron experiments may be useful to separate the longitudinal and transverse excitations. Recently, $\text{Cu}_2\text{CdB}_2\text{O}_6$ (Ref. 21) and $\text{Cu}_3\text{Mo}_2\text{O}_9$ (Ref. 22) were identified as realizations of the coupled dimers and chains models. Particularly, in the latter compound, the dimer energy is close to that of the chains, and more a complex physics is expected.

M. Matsumoto is greatly appreciated for fruitful discussion. This work was partly supported by Yamada Science Foundation, Asahi glass foundation, and Grant-in-Aid for Scientific Research (Grants No. 19740215 and No. 19052004) of Ministry of Education, Culture, Sports, Science and Technology of Japan.

*tmasuda@yokohama-cu.ac.jp

†Also at Condensed Matter Science Division, Oak Ridge National Laboratory, Oak Ridge, TN 37831-6393, USA.

¹T. Giamarchi and A. M. Tsvelik, Phys. Rev. B **59**, 11398 (1999).

²T. Nikuni, M. Oshikawa, A. Oosawa, and H. Tanaka, Phys. Rev. Lett. **84**, 5868 (2000).

³T. Giamarchi, C. Rugg, and O. Tchernyshev, Nat. Phys. **4**, 198 (2008).

⁴F. London, Nature (London) **141**, 643 (1938).

⁵J. D. Reppy and D. Depatte, Phys. Rev. Lett. **12**, 187 (1964).

⁶M. H. Anderson, J. R. Ensher, M. R. Matthews, C. E. Wieman, and E. A. Cornell, Science **269**, 198 (1995).

⁷R. Wynar, R. S. Freeland, D. J. Han, C. Ryu, and D. J. Heinzen, Science **287**, 1016 (2000).

⁸S.-k. Ma, C. Dasgupta, and C.-k. Hu, Phys. Rev. Lett. **43**, 1434 (1979).

⁹M. P. A. Fisher, P. B. Weichman, G. Grinstein, and D. S. Fisher, Phys. Rev. B **40**, 546 (1989).

¹⁰H. Manaka, A. V. Kolomiets, and T. Goto, Phys. Rev. Lett. **101**, 077204 (2008).

¹¹A. Oosawa and H. Tanaka, Phys. Rev. B **65**, 184437 (2002).

¹²T. Masuda, B. C. Chakoumakos, C. L. Nygren, S. Imai, and K. Uchinokura, J. Solid State Chem. **176**, 175 (2003).

¹³T. Masuda, A. Zheludev, B. Sales, S. Imai, K. Uchinokura, and S. Park, Phys. Rev. B **72**, 094434 (2005).

¹⁴T. Masuda, A. Zheludev, B. Grenier, S. Imai, K. Uchinokura, E. Ressouche, and S. Park, Phys. Rev. Lett. **93**, 077202 (2004).

¹⁵T. Masuda, K. Kakurai, M. Matsuda, K. Kaneko, and N. Metoki, Phys. Rev. B **75**, 220401(R) (2007).

¹⁶T. Masuda and G. J. Redhammer, Phys. Rev. B **74**, 054418 (2006).

¹⁷A. Zheludev, J. M. Tranquada, T. Vogt, and D. J. Buttrey, Phys. Rev. B **54**, 6437 (1996).

¹⁸M. Matsumoto, B. Normand, T. M. Rice, and M. Sigrist, Phys. Rev. B **69**, 054423 (2004).

¹⁹S. Sachdev and R. N. Bhatt, Phys. Rev. B **41**, 9323 (1990).

²⁰M. Matsumoto (private communication).

²¹M. Hase, M. Kohno, H. Kitazawa, O. Suzuki, K. Ozawa, G. Kido, M. Imai, and X. Hu, Phys. Rev. B **72**, 172412 (2005).

²²T. Hamasaki, T. Ide, H. Kuroe, T. Sekine, M. Hase, I. Tsukada, and T. Sakakibara, Phys. Rev. B **77**, 134419 (2008).